INTRODUCTION OF HETEROGENEOUS CELL PROPERTIES FOR MODELING EMERGENT STRESS FIELDS IN MULTICELLULAR SYSTEMS

Zachary E. Goldblatt (1), Heather A. Cirka (1), Habibeh Ashouri Choshali (2), Nima Rahbar (2),
Dannel McCollum (3), Kristen L. Billiar (1)

(1) Biomedical Engineering Worcester Polytechnic Institute Worcester, MA, USA (2) Civil Engineering Worcester Polytechnic Institute Worcester, MA, USA

(3) Biochemistry and Molecular Pharmacology UMASS Medical School Worcester, MA, USA

INTRODUCTION

In multicellular systems, cells interact with both their extracellular environment as well as neighboring cells. Collective cell behavior has been shown to affect cell behaviors including proliferation (1), morphology (2), and apoptosis (3). Cell-cell contact causes a transfer of forces between cells, which can influence cell behavior due to the stress field that they generate and in turn sense.

There is considerable interest in accurately modeling and calculating the stresses within cell monolayers to understand the underlying mechanical factors affecting cell behavior. Predicting the emergent stress fields is commonly performed with finite element models that simulate cell contractility as prestress or thermal cooling. Additionally, monolayer stress microscopy (MSM) is used for calculating cell-layer stresses from measured traction forces. Both predictions and calculations from TFM indicate high traction stresses in the substrate at the edges of the monolayers and high cell stresses in the central region of the cell layer.

In contrast, specific mechanosensitive biomarkers indicate high cell stresses on the periphery. For example, at the aggregate edge, alpha smooth muscle actin (α SMA), a contractile protein, is highest, apoptosis is lowest, and yes-associated protein (YAP) localizes to the nucleus (1,3,4).

We hypothesize that the discrepancy between predicted cell-layer stresses and measured stress-related biomarkers is the assumption of homogeneous contractile and mechanical properties throughout the cell layer utilized in current models and calculations. In this study, we model geometrically constrained cell monolayers with heterogeneous mechanical properties and compare the simulated and computed cell-layer stresses to stress-related biomarkers.

METHODS

Porcine valvular interstitial cells (VIC) were confined to microcontact printed circular collagen islands 200 μ m in diameter on 38.4kPa polyacrylamide (PA) gels prepared on glass coverslips. Factin, G-actin, and α SMA were stained via phalloidin, fluorescent DNase 1, and anti- α SMA respectively. Apoptosis and YAP presence were quantified via caspase-3/7 expression and anti-YAP, respectively.

For modeling of cell-layer stress, a thermal cooling finite element model of contraction was performed. Three distributions of contraction were modeled: 1) homogeneous coefficient of thermal expansion, 2) a step change heterogeneous model at half the radius of the aggregate, where the thermal expansion coefficient was reduced by 50%, and 3) an exponential distribution of thermal coefficient based on the measured distribution of cell spread area which is correlated with cell contraction in single-cell experiments (Fig. 2A). For calculation of cell-layer stress from measured traction forces, MSM was performed with three distributions of cell stiffness (modulus): 1) homogeneous, 2) step change in stiffness at half the radius, and 3) exponential distribution of stiffness (high at edge, low in center). Coefficient of thermal expansion was normalized so for each case, the integral of each curve would equal one another.

RESULTS

Protein markers associated with cell stress and contractility were first measured. It was found that the G-/F-actin ratio decreased radially from the center of aggregates to the edge in the center (Fig. 1A). We measured a doubling of α SMA integration into stress fibers from the center to the edge of aggregates (Fig. 1B). Additionally, we observed a steady decrease of apoptotic activity from 50% present in the aggregate center to nearly 0% present in the periphery (Fig. 1C).

Finally, we observed qualitatively YAP nuclear localization in peripheral cells and nuclear exclusion in central cells (Fig. 1D).



Figure 1: A) G/F-actin ratio decreases over aggregate radius. B) αSMA intensity increases with respect to aggregate radius. C) Cleaved caspase-3/7 presence decreases over aggregate radius. D) YAP nuclear localization is limited to edge cells. Scale bar=100μm.

The localization of our experimental biomarkers – higher G-actin in central region, higher αSMA incorporation into stress fibers along the edge, apoptosis occurrence in the center, and YAP localization along the periphery – suggest higher cell stress presence along the aggregate edges compared to the center.

For our homogeneous model, cell-layer stress is highest in the center and decreases towards the edge (Fig. 2B, 2D). In the heterogeneous step change model, the 50% reduction in contractility resulted in an opposite trend, where stress increases towards the edge. Finally, the continuous heterogeneous exponential model revealed an even more pronounced trend where circumferential stress is lowest in the center and increases towards the edge. The predicted substrate-level traction stresses were similar between all three conditions (Fig. 2C, 2D).

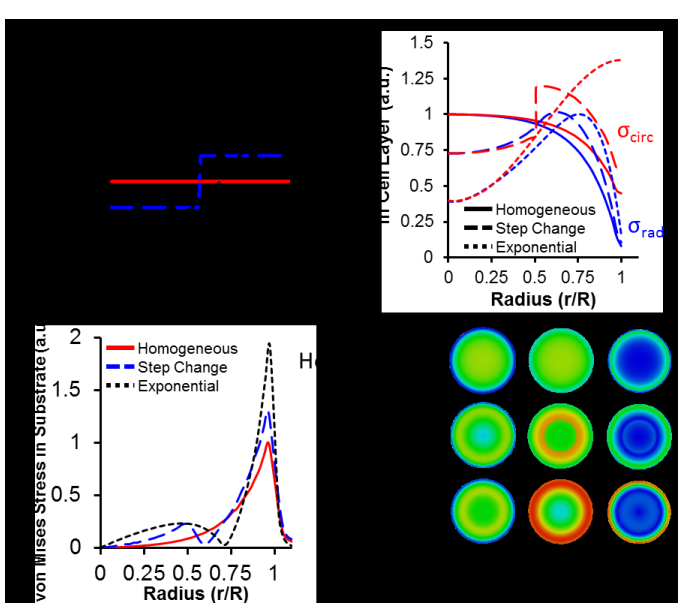


Figure 1: A) Coefficient of thermal expansion vs. radius.

Corresponds to cell area vs. radius, since cell area is linearly correlated with cell contraction in single-cell studies. B) Cell-layer radial (blue) and circumferential (red) stresses for three modeling conditions for contractility. C) Predicted von Mises stresses for three modeling conditions of cell contractility as a function of radius. D) Heat maps of predicted radial, circumferential, and traction stresses for all three conditions.

To calculate the cell-layer stress using MSM, measured substrate stresses from five different aggregates were averaged together to

obtain an average radial traction stress versus radius (Fig. 3A) and input into the finite element model to obtain radial and circumferential cell-layer stresses for an average aggregate (Fig. 3B). Once again, the homogeneous case showed highest cell-layer stress in the center and lowest on the edges, while both heterogeneous cases exhibited the opposite trend.

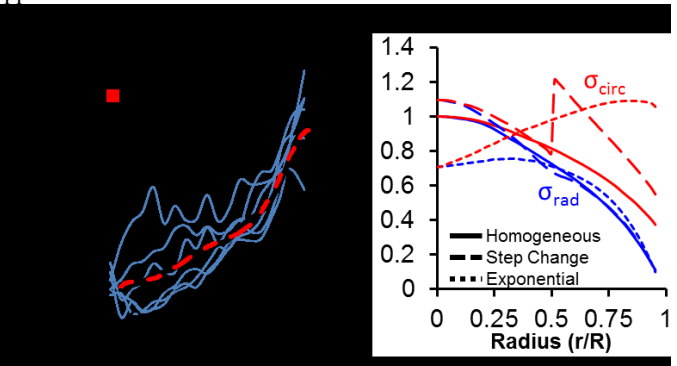


Figure 3: A) Average radial traction stresses measured from five aggregates were averaged (black line) and a best fit curve (red dashed). B) Cell-layer radial (blue) and circumferential (red) stresses for three modeling conditions cell stiffness.

DISCUSSION

Here, we have found that cell-layer stresses calculated with models incorporating *heterogeneous* contractile and mechanical properties better correlate with spatial distributions of measured stress-related biomarkers than models assuming homogeneous cell-layer properties. Homogeneous assumptions of mechanical properties led to predicted stresses that are opposite to those expected by the distribution of biomarkers.

These models show that even moderate changes in cellular contractility and stiffness can have drastic effects on the cell-layer stress distribution in confined multicellular systems. Additionally, the projected traction stresses have similar pattern for all conditions, which demonstrates the need for incorporating additional biophysical data (e.g., cell spread area, aspect ratio, etc.) into the models to accurate estimate the stress fields within the layers.

We present the first experimental evidence that supports that low stresses are experienced by central cells and is driving the biological response of aggregates. Our model improves upon previous models, however, it can still become more robust. We plan to obtain higher resolution biophysical data with validation to further alter cell contractility distributions and iterate our model's parameters. It is necessary to incorporate heterogeneous mechanical properties to accurately estimate the distribution of the emergent stress fields in our aggregates.

ACKNOWLEDGEMENTS

This work was funded in part by a National Science Foundation CMMI 1761432 and by a WPI-University of Massachusetts Medical School Seed Grant.

REFERENCES

- [1] Li, Bin et al., J. of Biomechanics, 42:1622–1627, 2009
- [2] He, Shijie et al., Biophysical Journal, 109:489-500, 2015
- [3] Cirka, Heather et al., Lab Chip, 17:814-829, 2017
- [4] Dupont, Sirio et al., Nature, 474:179-183, 2011
- [5] Chen, CS et al., Science, 276:1425-1428, 1997.
- [6] Zhang, YH et al., *Matrix Biol.*, 30:135-144, 2011